

A WASSERSTEIN GAN FOR JOINT LEARNING OF INPAINTING AND ITS SPATIAL OPTIMISATION

Pascal Peter

Mathematical Image Analysis Group, Faculty of Mathematics and Computer Science,
Campus E1.7, Saarland University, 66041 Saarbrücken, Germany.
peter@mia.uni-saarland.de

ABSTRACT

Classic image inpainting is a restoration method that reconstructs missing image parts. However, a carefully selected mask of known pixels that yield a high quality inpainting can also act as a sparse image representation. This challenging spatial optimisation problem is essential for practical applications such as compression. So far, it has been almost exclusively addressed by model-based approaches. First attempts with neural networks seem promising, but are tailored towards specific inpainting operators or require postprocessing. To address this issue, we propose the first generative adversarial network for spatial inpainting data optimisation. In contrast to previous approaches, it allows joint training of an inpainting generator and a corresponding mask optimisation network. With a Wasserstein distance, we ensure that our inpainting results accurately reflect the statistics of natural images. This yields significant improvements in visual quality and speed over conventional stochastic models and also outperforms current spatial optimisation networks.

Index Terms— inpainting, spatial optimisation, generative adversarial network, Wasserstein distance

1. INTRODUCTION

Image inpainting was originally introduced to restore missing or damaged image parts [2, 3]. In this classical setting, the known image data is predetermined. However, given the original image, one can instead consider a spatial optimisation problem: finding a fraction of known data that allows a high quality reconstruction of the image with inpainting. These sparse representations, the so-called inpainting masks, have practical applications such as inpainting-based compression [4, 5] and adaptive sampling [1]. Therefore, many sophisticated model-based approaches have been proposed for spatial inpainting data optimisation [6, 7, 8, 9, 10, 11, 12]. However, due to the unique challenges of this problem, solutions are often slow, complicated, or limited to specific inpainting operators.

Recently, some first attempts were made to solve the mask optimisation problem with neural networks [1, 13]. However, these approaches have limitations. From classical methods it is well known that optimal positions for an inpainting mask heavily depend on the inpainting operator. Despite this close connection, existing deep learning approaches do not allow to train a pair of inpainting and spatial optimisation networks, but either train them separately [1] or do not allow learned inpainting at all [13].

This work has received funding from the European Research Council (ERC) under the European Union’s Horizon 2020 research and innovation programme (grant agreement no. 741215, ERC Advanced Grant INCOVID). We thank Dai et al. [1] for providing their reference dataset.

1.1. Our Contribution

We propose the first generative adversarial approach for deep inpainting and spatial optimisation. It consists of three networks: an inpainting generator, a mask generator, and a discriminator. The discriminator allows our learned inpainting to approximate the statistics of natural images in terms of a Wasserstein distance, leading to convincing visual quality. Our mask network is the first to generate binary inpainting masks directly. It solves non-differentiability issues with approaches from neural network-based image compression. The combination of these ingredients makes effective joint learning of inpainting and mask optimisation possible.

1.2. Related Work

The selection of good known data is highly dependent on the inpainting operator. Only for individual operators such as homogeneous diffusion [14], true optimality statements have been proven [6], but even those can only be approximated in practice. Optimal control [8, 9, 10] approaches and a recent finite element method [12] offer good results, but are limited to certain operators. In our comparisons, we consider *probabilistic sparsification* (PS) and *non-local pixel exchange* (NLPE) [7] as representatives for classical methods. PS is a stochastic greedy method that gradually removes pixels which increase the inpainting error the least. NLPE is a postprocessing step, which moves mask points to the most promising positions of a randomly chosen candidate set. Together, they belong to the current state of the art in quality and are applicable to any deterministic inpainting operator. For a more detailed review of model-based spatial optimisation, we refer to Alt et al. [13].

To our best knowledge, only two deep learning approaches for spatial inpainting data optimisation exist so far. The network of Alt et al. [13] differs fundamentally from our approach in that it optimises masks for homogeneous diffusion inpainting, not for a deep inpainting. During training, the mask network feeds a non-binary confidence map for known data to a surrogate network approximating homogeneous diffusion. It requires postprocessing by stochastic sampling to obtain the final binary masks. The adaptive sampling contribution of Dai et al. [1] is closer in spirit to our approach: It combines a mask network *NetM* with a pre-trained inpainting network *NetE*. The authors note that joint training of *NetM* and *NetE* did not yield satisfying results due to the non-binary output of *NetM*. We address this in more detail in Section 3.1.

A full review of the numerous deep inpainting approaches is beyond the scope of this paper. Most of these focus on large hole inpainting [15, 16, 17], and methods for sparse data are much more rare [18, 19]. We explain in detail in Section 2, why we choose Wasserstein GANs [20, 19] as a foundation for our approach.

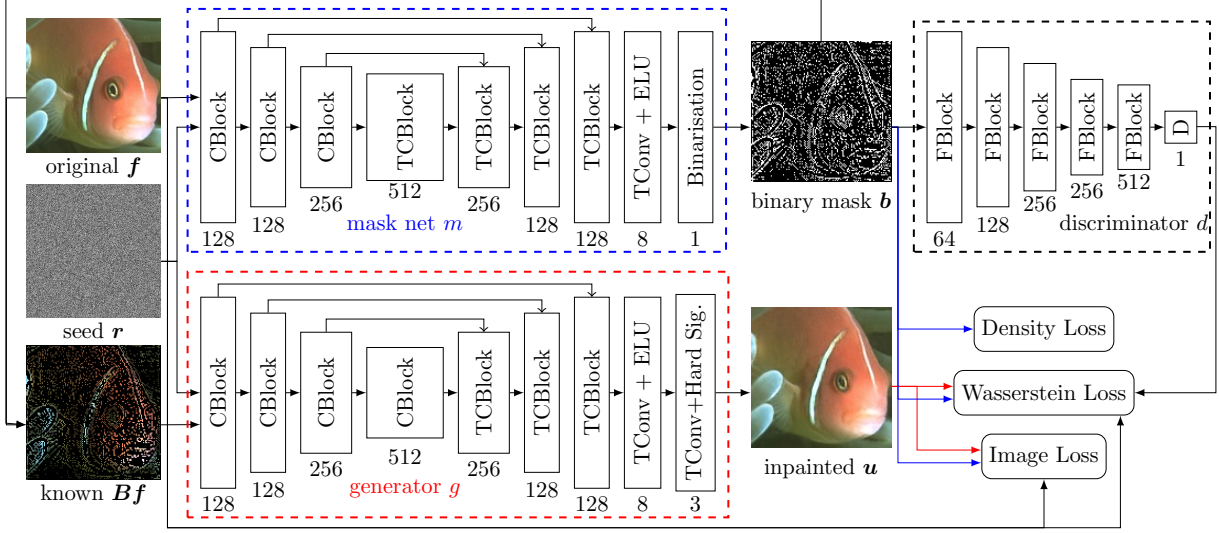


Fig. 1. Overview over our model structure. The arrows denote forward passes. CBLOCKS, TBLOCKS, and FBLOCKS denote convolutional, transposed convolutional, and funnel blocks (see Section 2), and TConv transposed convolutions. The block height visualises resolution and the block width roughly indicates the number of output channels, which is precisely given by the numbers below each block.

1.3. Organisation of the Paper

After a review of Wasserstein GANs in Section 2 we introduce our deep spatial optimisation approach in Section 3 and evaluate it in Section 4. The paper concludes with a discussion and outlook on future work in Section 5.

2. REVIEW: WASSERSTEIN GAN INPAINTING

Among classical inpainting techniques, those that accurately approximate the statistics of natural images [21] yield superior quality [5]. A consequent generalisation of this concept can be achieved by *generative adversarial networks* (GANs) [22]. A GAN relies on two competing networks to generate samples from a target distribution \mathbb{P}_t , which corresponds to the statistics of natural images in our case. The *generator* takes a sample from a source distribution \mathbb{P}_s , in our case a uniformly random distribution, and maps it to a representative of \mathbb{P}_t . The *discriminator* judges how well this representative fits to the target distribution. This creates a minmax problem, in which the generator tries to trick the discriminator in accepting its result as a true sample of \mathbb{P}_t .

Unfortunately, GANs tend to suffer from instabilities in training due to imbalances between the generator and the discriminator. Arjovsky et al. [20] have shown that the loss function, which measures the difference between generator samples and target distributions, has a large impact. Using a Wasserstein distance [23] instead of the classical Jensen-Shannon divergence [22] stabilises training, avoids vanishing gradients, and indicates training progress more reliably. Vařata et al. [19] have successfully applied *Wasserstein GANs* (WGANs) for image inpainting on random sparse data. Therefore, their architecture forms a good foundation for our own approach.

Assume we want to reconstruct an image of resolution $m \cdot n$ with k channels. We write its $N := mnk$ pixel values in vector notation as $\mathbf{f} \in \mathbb{R}^N$. Data is known at locations where the confidence function $\mathbf{c} \in [0, 1]^N$ is non-zero, thus providing side information for the generator $\mathbf{g} : (\mathbb{R}^N)^3 \rightarrow \mathbb{R}^N$, a parametric function represented by a network. Representing the known data as $\mathbf{C}\mathbf{f}$ with a masking

matrix $\mathbf{C} := \text{diag}(\mathbf{c}) \in \mathbb{R}^{N \times N}$, the generator creates the inpainting result $\mathbf{u} \in \mathbb{R}^N$ based on the inpainting constraint

$$\mathbf{u}(\mathbf{r}, \mathbf{c}, \mathbf{C}\mathbf{f}) := (\mathbf{I} - \mathbf{C})\mathbf{g}(\mathbf{r}, \mathbf{c}, \mathbf{C}\mathbf{f}) + \mathbf{C}\mathbf{f}. \quad (1)$$

The discriminator $d : \mathbb{R}^N \times \mathbb{R}^N \rightarrow \mathbb{R}$ aims to distinguish the distribution of the reconstruction with the known data as side information $\mathbb{P}(\mathbf{u}|\mathbf{c}, \mathbf{C}\mathbf{f})$ from the original distribution $\mathbb{P}(\mathbf{f}|\mathbf{c}, \mathbf{C}\mathbf{f})$, minimising

$$\mathbb{E}_{\mathbf{f} \sim \mathbb{P}_t, \mathbf{c} \sim \mathbb{P}_c} (d(\mathbf{f}, \mathbf{c}) - \mathbb{E}_{\mathbf{r} \sim \mathbb{P}_s} d(\mathbf{u}(\mathbf{r}, \mathbf{c}, \mathbf{C}\mathbf{f}), \mathbf{c})). \quad (2)$$

Here, \mathbf{f} is a sample from the natural image distribution \mathbb{P}_t , \mathbf{c} a random mask from the distribution \mathbb{P}_c , and \mathbf{r} a uniformly random seed. \mathbb{E} denotes the expected value which is estimated in practice via the batch mean. To approximate the Lipschitz property required by the Wasserstein distance, the discriminator weights are normalised to 1 in the 2-norm (see [19]). The generator has a combined loss which weights the discriminator opinion with parameter α against a mean absolute error (MAE) in terms of the 1-norm $\|\cdot\|_1$ that attaches the result to the concrete original image \mathbf{f} :

$$\mathbb{E}_{\mathbf{f} \sim \mathbb{P}_t, \mathbf{r} \sim \mathbb{P}_s, \mathbf{c} \sim \mathbb{P}_c} (-\alpha d(\mathbf{u}(\mathbf{r}, \mathbf{c}, \mathbf{C}\mathbf{f}), \mathbf{c}) + \|\mathbf{f} - \mathbf{u}(\mathbf{r}, \mathbf{c}, \mathbf{C}\mathbf{f})\|_1). \quad (3)$$

Regarding architecture, Vařata et al. [19] use a common hourglass structure for \mathbf{g} that successively subsamples the input data, passes it through a bottleneck and upsamples it again to the output (see \mathbf{g} in Fig. 1). Skip connections forward data between corresponding scales in this hierarchical network. Downsampling is performed by *CBLOCKS* using 3 parallel convolutions with filter size 5×5 , dilation rates 0, 2, and 5, and ELU activation. Their concatenated output is followed by a 2×2 max-pooling, which is the output of the block. Upsampling in *TCBLOCKS* follows the same principle with transposed convolutions and 2×2 upsampling instead. To restrict the image to the original pixel value range $[0, 1]$, the last transposed convolutional layer has a hard sigmoid activation. The discriminator follows a simpler downsampling architecture, where *FBLOCKS* combine 5×5 convolutions (stride 2) with Leaky ReLUs (see \mathbf{d} in Fig. 1). For exact details we refer to [19].

3. LEARNING MASKS WITH WASSERSTEIN GANS

3.1. Learning Binary Masks

Existing networks [1, 13] produce a non-binary confidence map $c \in [0, 1]^N$ during training. Dai et al. [1] have identified this as a major roadblock for joint training of an inpainting and mask networks. The known data Cf obtained in Eq. (1) provides information to the inpainting network that is not available during actual inpainting. Therefore, we need to binarise the mask already during training.

Unfortunately, binarisation is non-differentiable and thus prevents backpropagation. We solve this issue with a *binarisation block* for the last step of our mask generator. In a first step of this block, we apply a transposed convolution with a one channel output, followed by a hard sigmoid activation. We interpret the conversion of this non-binary output $c \in [0, 1]^N$ into a binary mask $b \in \{0, 1\}^N$ as an extreme case of quantisation. Such a discretisation of the co-domain restricts the admissible range of values, in our case just 0 and 1.

In deep compression, non-differentiability is often addressed by choosing representatives of the quantisation intervals according to additive random noise [24]. Theis et al. [25] have investigated different quantisation strategies in neural network-based compression and the impact of quantisation perturbations on training. Compared with additive noise and stochastic rounding they found hard rounding to perform the best. Therefore, we round non-binary confidence values c according to $b(c) = \lfloor c + 0.5 \rfloor$. Following the findings of Theis et al., we approximate the gradient of the binarisation layer by the derivative of a simple linear function for backpropagation.

3.2. Joint Learning of Inpainting Operator and Masks

The overall structure of our joint mask and inpainting WGAN is displayed in Fig. 1. Our new *mask generator* m maps the original $f \in \mathbb{R}^N$ and a uniformly random seed $r \in \mathbb{R}^N$ to a binary mask $b = m(r, f)$. The generator g uses this mask and the known data $Bf := \text{diag}(b)f$ as side information to create the inpainting result u from another random seed. The discriminator loss from Eq. 2 and the generator loss from Eq. 3 ensures that the inpainting respects the statistics of natural images. However, the mask c is replaced by the output b of the mask generator.

Unfortunately, we have no way to obtain training data for the unknown distribution of the binary masks that should be approximated by the mask generator m . This distribution depends on the inpainting operator which is simultaneously trained, thus creating a “chicken and egg” problem. We solve this by indirectly describing the distribution: The mask generator is coupled to the Wasserstein loss of the discriminator and generator, since b influences the inpainting result u . Moreover, we define a *density loss*, that measures the deviation of percentage of known pixels $\|b\|_1/N$ from the target density D of the inpainting mask. Directly, the following loss is imposed on the mask network, weighting the density loss against the inpainting MAE by β :

$$\mathbb{E}_{f \sim \mathbb{P}_t, r \sim \mathbb{P}_s} (\|m(r, f)\|_1/N - D | + \beta \|f - u(r, m(r, f), Bf)\|_1). \quad (4)$$

The architecture of the generator and discriminator is identical to the one from Section 2. The mask generator mostly follows the inpainting generator design. We only replace the last block by the binarisation from Section 3.1. Due to the Wasserstein loss, training is straightforward: In each epoch, we update the weights of all three networks with backpropagation. Training remains stable and requires no fine tuning of the generator/discriminator balance.

Density	PS	PS+NLPE	MG
5%	13.98	10.98	11.19
10%	9.08	7.51	8.87
20%	5.19	4.31	6.70

Table 1. MAE Comparison to Stochastic Methods. Our mask GAN (MG) outperforms probabilistic sparsification (PS) consistently and is competitive with non-local pixel exchange (NLPE) on low densities.

Density	PS	PS+NLPE	MG (CPU)	MG (GPU)
5%	58.84	251.28	0.93	0.031
10%	33.89	340.61	0.93	0.031
20%	18.86	389.34	0.93	0.031

Table 2. Runtime Comparison on 128×128 images with an Intel Core i56660K@3.50GHz and a NVIDIA Geforce GTX 1070. Our WGAN is faster than classical methods by several orders of magnitude. Its runtime is independent of the mask density.

4. EXPERIMENTS

4.1. Experimental Setup

We compare our mask Wasserstein-GAN (MG) against probabilistic mask techniques [7], and the neural network NetM by Dai et al. [1].

Our neural networks were trained on a 100,000 image *ImageNet* subset of Dai et al. [1] and the corresponding validation set. Depending on the evaluation set, these were centre-cropped to either 128×128 or 64×64 . We used the *Adam* optimiser [29] with learning rate $5 \cdot 10^{-5}$ and a batch size of $b = 32$ for image size 128×128 , and $b = 128$ for image size 64×64 . The model parameters were set to $\alpha = 0.005$ and $\beta = 1$. For each mask density D , separate networks were trained. We chose the best weights w.r.t. the mask validation loss from Eq. (4) after 1000 epochs. In most cases, this was already reached after ≈ 100 epochs.

As evaluation datasets we use the ImageNet test set provided by Dai et al. [1] for the network comparison. For the comparison with NLPE, we use the Berkeley shape database *BSDS500* [30], since it has better public availability and this also demonstrates that our networks transfer well to other natural image databases.

4.2. Comparison Against Probabilistic Methods

Probabilistic sparsification (PS) with a non-local pixel exchange (NLPE) as a postprocessing step defines a benchmark for the best results obtainable so far with homogeneous diffusion inpainting. Other methods such as the network of Alt et al. [13] or optimal control [8, 9, 10] yield comparable quality.

We optimise the stochastic models for MAE since this is also part of the network loss. NLPE uses 5 cycles of $|c|$ iterations. At first glance, in terms of MAE, our mask GAN (MG) is situated in-between PS and PS+NLPE in Table 1. It performs better on sparser masks which are more relevant for e.g. compression applications and comes very close to the NLPE error for 5%. Note, however, that the MAE does not accurately reflect the Wasserstein loss. The visual comparison in Fig. 2 demonstrates that our approach of approximating natural image statistics yields perceptually more pleasing results, even at the same MAE in image (b). In particular, our mask approach can reconstruct image features such as the straight lines in Fig. 2(a) from less known data. This allows our MG to distribute the known data much more evenly over the image than the classical methods.

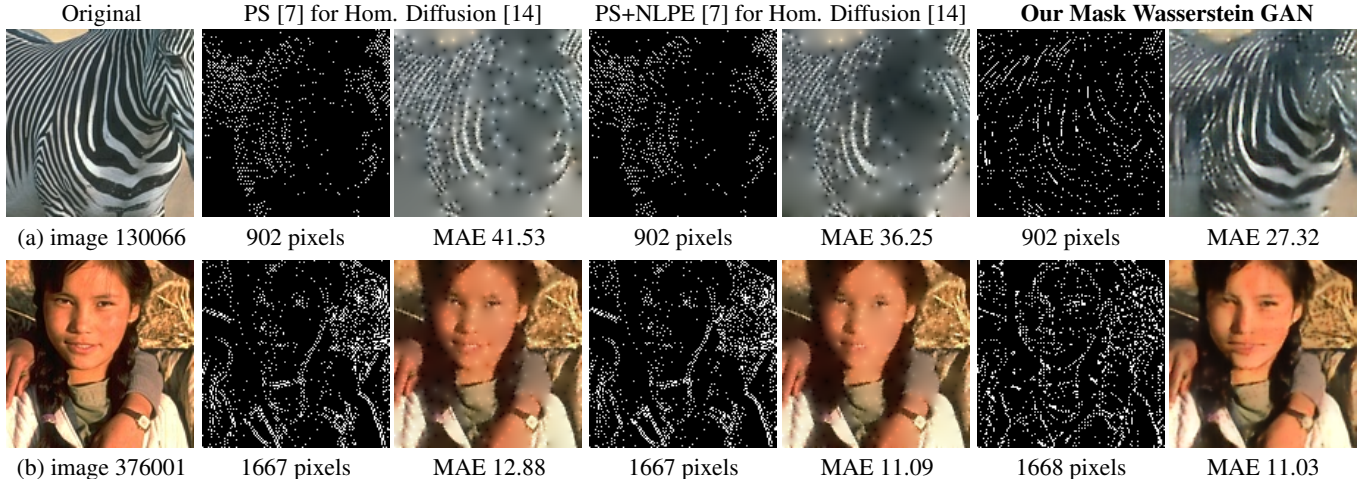


Fig. 2. Visual Comparison to Probabilistic Methods. Known data points are marked in white. Our mask WGAN reconstructs structures from less clustered data and does not suffer from visual artefacts such as singularities.

Density	NetE rand [1]	WGAN rand [19]	NetM/NetE [1]	NetM/CDD [26]	NetM/BPFA [27]	NetM/MS [28]	Our MG
5%	18.44	18.85	20.35	20.22	15.82	20.70	21.66
10%	19.94	20.78	21.93	22.42	20.82	22.98	23.63
20%	22.06	22.95	24.31	24.38	24.16	25.04	25.36

Table 3. PSNR Comparison Against NetM. Our MWG approach outperforms NetM in combination with all four inpainting operators investigated by Dai et al. [1]. In particular, it can outperform the full network approach with NetE by more than 1db in PSNR, even though MWG does not minimise PSNR.

They tend to cluster known pixels left and right to edges in accordance to the theoretical results of Belhachmi et al. [6].

In addition to the better visual quality, our Mask GAN is also substantially faster than a PS/NLPE conjugate-gradient implementation with relative residual 10^{-6} . On a single CPU core, the speed-up reaches up to a factor ≈ 63 w.r.t. PS and a factor ≈ 419 w.r.t. NLPE. With GPU support, our GAN can be up to $\approx 12,560$ times faster. Note that faster model-based alternatives to PS exist [6, 12], however they need post processing to achieve the quality of PS+NLPE.

4.3. Comparison Against NetM

In a second set of experiments, we compare against the mask generator NetM [1] on the test set curated by Dai et al. It consists of 1000 64×64 images. They provide peak-signal-to-noise ratio (PSNR) results of NetM in combination with the corresponding inpainting network NetE and multiple classical inpainting approaches [26, 28, 27]. Note that NetM is trained to minimise a 2-norm, giving it an advantage over our 1-norm/Wasserstein trained MG. Nevertheless, in Table 3, MG outperforms NetM+NetE by up to 1.7 dB.

To verify that this advantage does not only result from using a GAN for inpainting, we also compare the inpainting WGAN [19] to NetE on random masks. On 5% known data, the WGAN outperforms NetE only by 0.4 dB. Our mask GAN increases this improvement over NetM+NetE to 1.3 dB. This indicates that our mask binarisation and joint training offers an advantage.

Additional inpainting operators in combination with NetM, such as the Bayesian beta process factor analysis (BPFA) [27], curvature-driven diffusion (CCD) [26], or Mumford-Shah (MS) inpainting [28] all yield worse results than our mask GAN. We outperform the best

NetM approach by up to 0.96 dB.

5. CONCLUSION AND FUTURE WORK

We have presented the first adversarial network for joint learning of a generative inpainting operator and a binary mask generator. With a mathematically well-founded Wasserstein framework, our inpainting GAN approximates the statistics of natural images, yielding visual improvements over model-based stochastic approaches with homogeneous diffusion. Simultaneously, our approach is faster by several orders of magnitude. It also qualitatively outperforms competing neural networks for spatial optimisation in combination with many inpainting operators.

Currently, we are working on further refinements of both the general framework and the concrete network architecture. Moreover, we plan to evaluate the impact of individual components with an extended evaluation and ablation study in the future. Our model is a step towards fast, visually accurate, and mathematically justified spatial optimisation with deep learning. We hope that it contributes to practical applications such as image compression or adaptive sampling in the future.

6. REFERENCES

- [1] Q. Dai, H. Chopp, E. Pouyet, O. Cossairt, M. Walton, and A. K. Katsaggelos, "Adaptive image sampling using deep learning and its application on X-Ray fluorescence image reconstruction," *IEEE Transactions on Multimedia*, vol. 22, no. 10, pp. 2564–2578, Dec. 2019.

- [2] S. Masnou and J.-M. Morel, "Level lines based disocclusion," in *Proc. 1998 IEEE International Conference on Image Processing*, Chicago, IL, Oct. 1998, vol. 3, pp. 259–263.
- [3] M. Bertalmío, V. Caselles, S. Masnou, and G. Sapiro, "Inpainting," in *Computer Vision: A Reference Guide*, K. Ikeuchi, Ed., pp. 401–416. Springer, New York, 2014.
- [4] I. Galić, J. Weickert, M. Welk, A. Bruhn, A. Belyaev, and H.-P. Seidel, "Image compression with anisotropic diffusion," *Journal of Mathematical Imaging and Vision*, vol. 31, no. 2–3, pp. 255–269, July 2008.
- [5] C. Schmaltz, P. Peter, M. Mainberger, F. Ebel, J. Weickert, and A. Bruhn, "Understanding, optimising, and extending data compression with anisotropic diffusion," *International Journal of Computer Vision*, vol. 108, no. 3, pp. 222–240, July 2014.
- [6] Z. Belhachmi, D. Bucur, B. Burgeth, and J. Weickert, "How to choose interpolation data in images," *SIAM Journal on Applied Mathematics*, vol. 70, no. 1, pp. 333–352, 2009.
- [7] M. Mainberger, S. Hoffmann, J. Weickert, C. H. Tang, D. Johannsen, F. Neumann, and B. Doerr, "Optimising spatial and tonal data for homogeneous diffusion inpainting," in *Scale Space and Variational Methods in Computer Vision*, A. M. Bruckstein, B. ter Haar Romeny, A. M. Bronstein, and M. M. Bronstein, Eds., vol. 6667 of *Lecture Notes in Computer Science*, pp. 26–37. Springer, Berlin, 2012.
- [8] L. Hoeltgen, S. Setzer, and J. Weickert, "An optimal control approach to find sparse data for Laplace interpolation," in *Energy Minimisation Methods in Computer Vision and Pattern Recognition*, A. Heyden, F. Kahl, C. Olsson, M. Oskarsson, and X.-C. Tai, Eds., vol. 8081 of *Lecture Notes in Computer Science*, pp. 151–164. Springer, Berlin, 2013.
- [9] Y. Chen, R. Ranftl, and T. Pock, "A bi-level view of inpainting-based image compression," in *Proc. 19th Computer Vision Winter Workshop*, Z. Kúkelová and J. Heller, Eds., Křtiny, Czech Republic, Feb. 2014.
- [10] S. Bonettini, I. Loris, F. Porta, M. Prato, and S. Rebegoldi, "On the convergence of a linesearch based proximal-gradient method for nonconvex optimization," *Inverse Problems*, vol. 33, no. 5, pp. 055005, Mar. 2017.
- [11] L. Karos, P. Bheed, P. Peter, and J. Weickert, "Optimising data for exemplar-based inpainting," in *Advanced Concepts for Intelligent Vision Systems*, J. Blanc-Talon, D. Helbert, W. Philips, D. Popescu, and P. Scheunders, Eds., vol. 11182 of *Lecture Notes in Computer Science*, pp. 547–558. Springer, Cham, 2018.
- [12] V. Chizhov and J. Weickert, "Efficient data optimisation for harmonic inpainting with finite elements," in *Computer Analysis of Images and Patterns*, N. Tsapatsoulis, A. Panayides, T. Theo, A. Lanitis, and C. Pattichis, Eds., vol. 13053 of *Lecture Notes in Computer Science*. Springer, Cham, 2021.
- [13] T. Alt, J. Weickert, and P. Peter, "Learning sparse masks for diffusion-based image inpainting," arXiv:2110.02636 [eess.IV], Oct. 2021.
- [14] T. Iijima, "Basic theory on normalization of pattern (in case of typical one-dimensional pattern)," *Bulletin of the Electrotechnical Laboratory*, vol. 26, pp. 368–388, 1962, In Japanese.
- [15] J. Xie, L. Xu, and E. Chen, "Image denoising and inpainting with deep neural networks," in *Proc. 26th International Conference on Neural Information Processing Systems*, Lake Tahoe, NV, Dec. 2012, pp. 350–358.
- [16] D. Pathak, P. Krähenbühl, J. Donahue, T. Darrell, and A. A. Efros, "Context encoders: Feature learning by inpainting," in *Proc. 2016 IEEE Conference on Computer Vision and Pattern Recognition*, Las Vegas, NV, June 2016, pp. 2536–2544.
- [17] H. Liu, B. Jiang, Y. Xiao, and C. Yang, "Coherent semantic attention for image inpainting," in *Proc. 2019 IEEE/CVF International Conference on Computer Vision*, Seoul, Korea, Oct. 2017, pp. 4170–4179.
- [18] D. Ulyanov, A. Vedaldi, and V. Lempitsky, "Deep image prior," in *Proc. 2018 IEEE Conference on Comp. Vis. and Pattern Recognition*, Salt Lake City, UT, June 2018, pp. 9446–9454.
- [19] D. Vařata, T. Halama, and M. Friedjungová, "Image inpainting using Wasserstein generative adversarial imputation network," in *Proc. 30th International Conference on Artificial Neural Networks*, Sept. 2021, pp. 575–586.
- [20] M. Arjovsky, S. Chintala, and L. Bottou, "Wasserstein generative adversarial networks," in *Proc. 34th International Conference on Machine Learning*, D. Precup and Y. W. Teh, Eds., Sydney, Australia, Aug. 2017, vol. 70 of *Proceedings of Machine Learning Research*, pp. 214–223.
- [21] P. Peter and J. Weickert, "Compressing images with diffusion- and exemplar-based inpainting," in *Scale Space and Variational Methods in Computer Vision*, J.-F. Aujol, M. Nikolova, and N. Papadakis, Eds., vol. 9087 of *Lecture Notes in Computer Science*, pp. 154–165. Springer, Berlin, 2015.
- [22] I. Goodfellow, J. Pouget-Abadie, M. Mirza, B. Xu, D. Warde-Farley, S. Ozair, A. Courville, and Y. Bengio, "Generative adversarial nets," *Advances in Neural Information Processing Systems*, vol. 27, pp. 2672–2680, Dec. 2014.
- [23] L. N. Vaserstein, "Markov processes over denumerable products of spaces, describing large systems of automata," *Problemy Peredachi Informatsii*, vol. 5, no. 3, pp. 64–72, Feb. 1969.
- [24] J. Ballé, V. Laparra, and E. P. Simoncelli, "End-to-end optimised image compression," in *Proc. 5th International Conference on Learning Representations*, Toulon, France, Apr. 2017.
- [25] L. Theis, W. Shi, A. Cunningham, and F. Huszár, "Lossy image compression with compressive autoencoders," in *Proc. 5th International Conference on Learning Representations*, Toulon, France, Apr. 2016.
- [26] T. F. Chan and J. Shen, "Non-texture inpainting by curvature-driven diffusions (CDD)," *Journal of Visual Communication and Image Representation*, vol. 12, no. 4, pp. 436–449, 2001.
- [27] M. Zhou, H. Chen, J. Paisley, L. Ren, L. Li, Z. Xing, D. Dunson, G. Sapiro, and L. Carin, "Nonparametric Bayesian dictionary learning for analysis of noisy and incomplete images," *IEEE Transactions on Image Processing*, vol. 21, no. 1, pp. 130–144, Jan. 2011.
- [28] S. Eshedoglu and J. Shen, "Digital inpainting based on the Mumford–Shah–Euler image model," *European Journal of Applied Mathematics*, vol. 13, no. 4, pp. 353–370, Aug. 2002.
- [29] D. P. Kingma and J. Ba, "Adam: A method for stochastic optimization," in *Proc. 3rd International Conference on Learning Representations*, San Diego, CA, May 2015.
- [30] P. Arbelaez, M. Maire, C. Fowlkes, and J. Malik, "Contour detection and hierarchical image segmentation," *IEEE Transactions on Pattern Analysis and Machine Intelligence*, vol. 33, no. 5, pp. 898–916, Aug. 2011.